Enhanced Electro-Optic Modulator Performance on Indium Phosphide Platform Using n-p-i-n Stack

J. A. Hillier, A. K. Sünnetçioğlu, D. Fernandes da Silva, and W. Yao.

Eindhoven Hendrik Casimir Institute, Eindhoven University of Technology, Eindhoven, The Netherlands.

We investigate the modification of the layer stack in co-planar strip (CPS) Mach-Zehnder modulators (MZMs) on the indium phosphide (InP) platform, replacing the conventional p-i-n layer stack with an n-p-i-n configuration to reduce optical and electrical losses while improving the overlap between electric and optical fields. We present simulations of the electric field distribution across the waveguide layer stack as a function of the applied voltage, performed by solving Poisson-current equations, and demonstrate that the n-p-i-n stack reduces V_π *by ~10% and increases the electric bandwidth significantly, owing to the reduction in the electronic losses. This work provides a pathway to enhance the performance of InP-based MZMs.*

Introduction

Advancements in indium phosphide (InP)-based Mach-Zehnder modulators (MZMs) have enabled high-speed optical communications, achieving bandwidths up to 100 GHz and data transmission rates of 320 Gbit/s [1–3]. These modulators utilise a co-planar strip (CPS) design on a generic InP platform, which allows for compact device footprints and reduced microwave losses while maintaining high bandwidth and compatibility with generic foundry processes. However, a significant challenge remains in the relatively high half-wave voltage-length product ($V_\pi L$) of 0.8 Vcm, requiring prohibitive driving systems with high speed and peak-peak voltage driving while also increasing the power consumption of the device. To address this limitation, it is essential to enhance the electro-optic efficiency of the MZMs, thereby reducing V_π. One promising approach is to modify the layer stack of the waveguide by replacing the conventional p-i-n configuration with an n-p-i-n structure. This concept has been explored by researchers at NTT [1,2], who demonstrated that the n-p-i-n stack reduces radiofrequency (RF) losses, increasing the available bandwidth, as well as optical losses and improved overlap between optical and electronic fields, giving way to a lower V_π. In this work, we investigate the implementation of an n-p-i-n layer stack in the CPS-MZM design on the InP platform. We seek to merge the advantages of the JePPIX generic platform [3,4] with the benefits of the n-p-i-n configuration used by NTT. We solve the Poisson-Current equations [5] to obtain the electric field distribution across the waveguide layer stack as a function of the applied voltage. We then analyse the overlap between the electric field and the optical mode to assess the improvement in electro-optic efficiency. Finally, we utilise an equivalent circuit modelling approach [6,7] to extract the small-signal electric-electric (EE) frequency response of the CPS transmission line. Our results indicate that the n-p-i-n layer stack significantly reduces V_π, thereby enhancing the modulator's performance. This modification provides a pathway to overcome the limitations imposed by high half-wave voltages while simultaneously offering significant gains to the EE bandwidth. The findings of this study contribute to the development of more efficient and high-speed InP-based MZMs for high-speed optical communication systems.

n-p-i-n Layer Stack Concept

The conventional design of InP-based Mach-Zehnder modulators employs a p-i-n layer stack, where the non-intentionally doped layer, potentially comprising of multiple quantum wells (MQWs), is sandwiched between p-type and n-type cladding layers. To enhance the modulator's performance, we explore the use of an n-p-i-n layer stack, as has been proposed by researchers at NTT [1,2]. In this configuration, the n-type buffer layer above the non-intentionally doped layer is replaced with a p-type buffer layer while the upper layers are instead n-type. The intent of the design is to reduce the electronic losses in the top layers, owing to the larger mobility of the carriers and thus conductivity of the n-doped InP and InGaAs in comparison to the p-type. The higher carrier mobility inherent to n-type InP also reduces the optical losses for the parts of the optical mode that overlap with the two top layers. Finally, the shift of the p-n junction closer to the MQWs brings the depletion zone closer to the peak of the optical mode, improving the overlap between the electric field and the optical mode. The depletion region growth into the MQW layers is vital for higher EO efficiency, as the unintentional doping of the MQW layers leads to the MQW layer not being truly intrinsic outside of the depletion region, limiting the electric field drop across the layer containing the bulk of the optical mode. Figure 1 illustrates the cross-sectional schematics of the CPS design with both (a) the conventional p-i-n stack and (b) the proposed n-p-i-n stack. The schematics show the thicknesses of each layer. The initial investigations outlined in this work do not alter the layer thicknesses from the generic layer stack utilised in previous research [8,9].

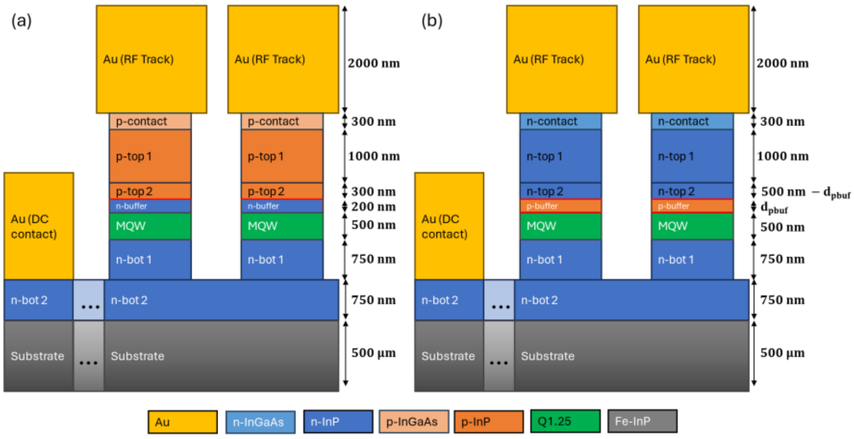

Figure 1. Cross-sectional schematics of the CPS design with (a) p-(n)i-n layer stack and (b) n-p-i-n layer stack, showing layer doping types and thicknesses.

Simulation Methodology

To evaluate the performance improvements offered by the n-p-i-n layer stack, we performed simulations to obtain the electric field distribution across the waveguide layer stack as a function of the applied voltage. The simulations were conducted using NextNano software [10], which solves the Poisson-current equations for semiconductor devices. The simulation domain included the full cross-section of the waveguide, incorporating all relevant layers with their respective doping concentrations and material properties. For both the p-i-n and n-p-i-n configurations, we simulated the electric field profiles, $\mathrm{E}(\mathrm{z})$, across the depth of the layer stack. To study the effect on V_{π}, we study the 2D overlap integral $\Gamma(z)$ (Eq. 1) in both configurations, which quantifies the interaction between the electric field profile and the optical mode defined by a central position z_0 and radius $\mathrm{r}_{\mathrm{opt}}$.

$$\Gamma(z) = \int_{-\infty}^{\infty} \left(\frac{E(z)}{\int_{-\infty}^{\infty} (|E(z)|^2 dz)} \right) \left(\sqrt{\frac{2}{\pi}} e^{-\frac{(z-z0)^2}{2 r_{opt}^2}} \right) dz \tag{1}$$

The simulations give the electron and hole densities and mobility as a function of the depth below the metal layer, z. These values are used to calculate the conductivity of each 'slice', $\sigma_{sl} = 1/\rho_{sl}$, that is used to calculate the impedance of a lumped circuit element, comprising a parallel resistor and capacitor with per-unit-length resistance and capacitance $R' = \rho_{sl} d_{sl}/w_{wvg}$ and $C' = \varepsilon_{sl} w_{wvg}/d_{sl}$, respectively, where ε_{sl} and d_{sl} are the permittivity and thickness of the slice while w_{wvg} is the waveguide width, taken to be 1.0 µm [11]. Treating the waveguide stack as a combination of each lumped circuit element in series provides the impedance of the entire waveguide stack. This impedance is fed into an equivalent circuit model, following the application of Kirchhoff's rules and considerations of the device geometry to produce lumped elements comprising a simple transmission line, allowing one to calculate the propagation constant, γ_{RF}, and the S-parameters of the transmission line [12]. This work expands upon previous implementations of the equivalent circuit modelling approach [13,14] by replacing analytical methods and for determining the depletion zone using design-based intended layers with the more realistic outputs of the NextNano simulation. This is vital to model the more complex behaviour of the depletion zone within the n-p-i-n layer stack.

Results and Discussion

Figure 2 shows the electric field distribution across the layer depth for (a) the p-i-n stack and (b) the n-p-i-n stack. The parameters defining the optical mode were taken from previous studies utilising an optical mode solver [15]. The optical mode profile is superimposed onto the electric field distribution to qualitatively assess the overlap between the two fields. We observe that in the p-i-n configuration at zero bias voltages, the electric field is concentrated near the p-n junction, with limited overlap with the optical mode. Increasing the reverse bias voltage extends the depletion zone further into the non-intentionally doped layer, increasing the relative concentration of the electric field within this layer. The peak electric field is felt within the n-buffer layer, which exist where the optical mode is weaker. In contrast, the n-p-i-n stack exhibits an electric field that extends more uniformly across the MQW layer, where the optical mode is primarily confined. The calculated overlap integrals for both configurations are presented in Figure 3. The simulations indicate a boost in the 2D overlap integral for a reverse bias voltage of 4 V from 70% in the p-i-n stack to 80% in the n-p-i-n stack.

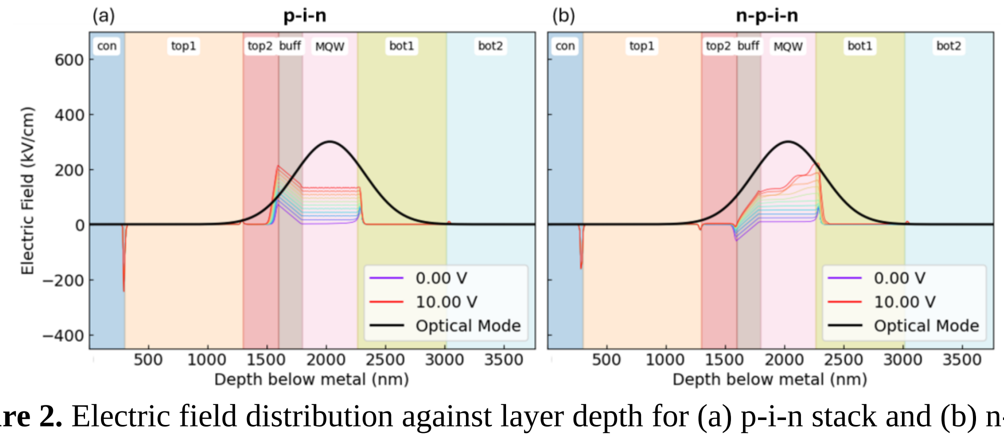

Figure 2. Electric field distribution against layer depth for (a) p-i-n stack and (b) n-p-i-n stack, with superimposed optical mode profile.

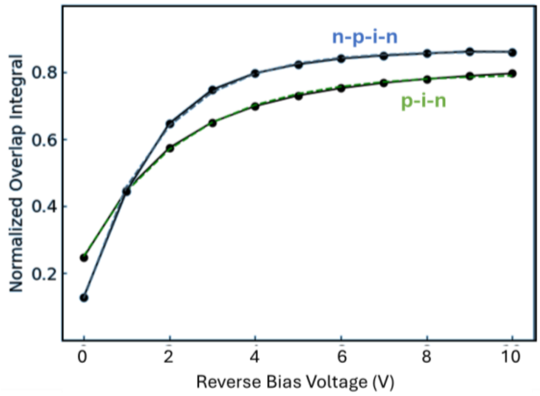

Figure 3. Normalised overlap integral against the applied reverse bias voltage for the p-i-n (green) and n-p-i-n (blue) layer stacks.

Figure 4 presents the simulated EE S_{21} parameters for the (a) p-i-n and (b) n-p-i-n layer stacks for a swept reverse bias voltage from 0 V to 10 V (purple-red lines). The black horizontal lines indicate where $S_{21} = 0$ dB and $S_{21} = -6$ dB, used to estimate the -6 dB EE bandwidth. For the p-i-n stack, the lack of a sufficient depletion zone within the material due to the built-in-potential is reflected in the poor EE bandwidth when operated at 0 V. However, even small increases in the applied reverse bias voltage dramatically extend the bandwidth (from ~50 GHz to ~150 GHz). For the transmission line based on the n-p-i-n layer stack, the bandwidth at 0 V is already at the 150 GHz mark, and, given the assumed device geometry ($l_{ps} = 1$ mm, $w_{wvg} = 1$ µm, $w_{sig} = 10$ µm, $w_{s2s} = 7$ µm) and likely unphysical sharp step-based doping profiles utilised in this study, is increased to beyond 200 GHz for higher reverse bias voltages.

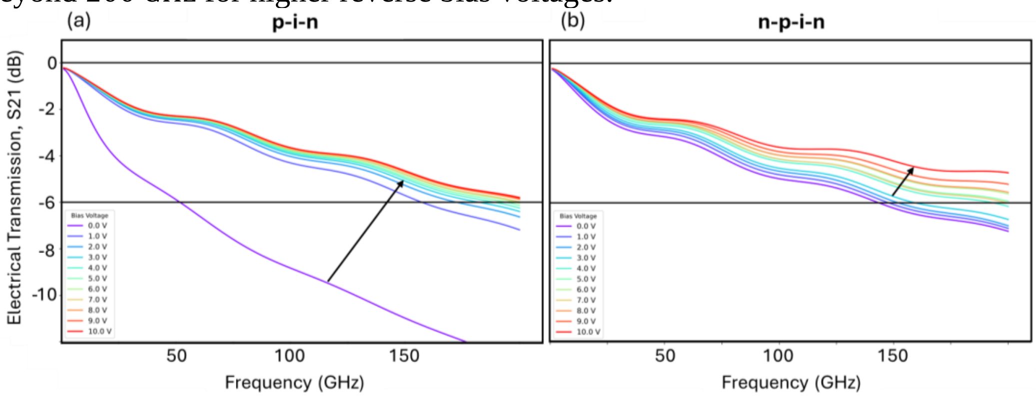

Figure 4. Simulated EE S_{21} parameters for the (a) p-i-n and (b) n-p-i-n layer stacks for a swept reverse bias voltage from 0 V to 10 V (purple-red lines in rainbow order). The black horizontal lines indicate where $S_{21} = 0$ dB and $S_{21} = -6$ dB.

Conclusions

We investigated the modification of the layer stack in InP-based CPS Mach-Zehnder modulators by replacing the conventional p-i-n configuration with an n-p-i-n structure. Through simulations of the current-Poisson equations and equivalent circuit modelling of the transmission line based on the CPS-MZM design, we demonstrated that the n-p-i-n stack enhances both the electro-optic efficiency and bandwidth of the modulator. . The n-p-i-n layer stack provides a viable pathway to overcome the limitations of the conventional p-i-n design, contributing to the advancement of InP-based integrated photonics.

References

[1] J. A. Hillier, A. Meighan, M. Van Den Hout, S. Van Der Heide, S. Cakmakyapan, W. Yao, R. Van Dommele, M. Wale, C. Okonkwo, and K. Williams, "A 100 GBaud co-planar stripline Mach-Zehnder modulator on Indium Phosphide platform," in 2023 Opto-Electronics and Communications Conference (OECC) (IEEE, 2023), pp. 1–3.

[2] A. Meighan, W. Yao, M. J. Wale, and K. A. Williams, "Design of 100 GHz-class Mach-Zehnder modulators in a generic indium phosphide platform," in 2020 IEEE Photonics Conference (IPC) (IEEE, 2020), pp. 1–2.

[3] J. A. Hillier, Q. Hu, H. Chen, A. Meighan, L. Augustin, M. Wale, K. Williams, and W. Yao, "A Co-planar Stripline Mach-Zehnder Modulator Enabling 160 GBd PAM-4 on an Indium Phosphide Platform," in Optical Fiber Communication Conference (OFC) 2024 (Optica Publishing Group, 2024), p. Tu2D.4.

[4] J. Ozaki, Y. Ogiso, Y. Hashizume, H. Yamazaki, K. Nagashima, N. Nunoya, and M. Ishikawa, "Over-85-GHz-Bandwidth InP-Based Coherent Driver Modulator Capable of 1-Tb/s/λ-Class Operation," Journal of Lightwave Technology 41, 3290–3296 (2023).

[5] Y. Ogiso, Y. Hashizume, H. Tanobe, N. Nunoya, M. Ida, Y. Miyamoto, M. Ishikawa, J. Ozaki, Y. Ueda, H. Wakita, M. Nagatani, H. Yamazaki, M. Nakamura, T. Kobayashi, and S. Kanazawa, "80-GHz Bandwidth and 1.5-V Vπ InP-Based IQ Modulator," Journal of Lightwave Technology 38, 249–255 (2020).

[6] K. Lawniczuk and M. K. Smit, "JePPIX: access to generic foundry processes for InP photonic integrated circuits," in 2014 IEEE Avionics, Fiber-Optics and Photonics Technology Conference (AVFOP) (IEEE, 2014), pp. 43–44.

[7] "JePPIX Platform for Photonic Integration Homepage," https://www.jeppix.eu/.

[8] M. N. Darwish, J. L. Lentz, M. R. Pinto, P. M. Zeitzoff, T. J. Krutsick, and Hong Ha Vuong, "An improved electron and hole mobility model for general purpose device simulation," IEEE Trans Electron Devices 44, 1529–1538 (1997).

[9] W. Yao, G. Gilardi, M. K. Smit, and M. J. Wale, "Equivalent circuit modelling of integrated traveling-wave optical modulator in InP foundry platform," in 18th European Conference on Integrated Optics (ECIO 2016) (2016), pp. 1–2.

[10] H. Yu and W. Bogaerts, "An Equivalent Circuit Model of the Traveling Wave Electrode for Carrier-Depletion-Based Silicon Optical Modulators," Journal of Lightwave Technology 30, 1602–1609 (2012).

[11] S. Birner, T. Zibold, T. Andlauer, T. Kubis, M. Sabathil, A. Trellakis, and P. Vogl, "nextnano: General Purpose 3-D Simulations," IEEE Trans Electron Devices 54, 2137–2142 (2007).

[12] W. Yao, "Towards a High-Capacity Multi-Channel Transmitter in Generic Photonic Integration Technology," Thesis, Eindhoven University of Technology (2016).

[13] J. A. Hillier, W. Yao, M. J. Wale, and K. A. Williams, "Equivalent circuit modelling of coplanar waveguide InP electro-optic phase modulators," in Proceedings of the 26th Annual Symposium of the IEEE Photonics Benelux Chapter 2022 Institute of Electrical and Electronics Engineers. (n.d.).

[14] J. A. Hillier, M. J. Wale, K. A. Williams, and W. Yao, "Equivalent circuit modelling of high-speed coplanar strip InP-based Mach-Zehnder phase modulators ," in Proceedings of the 26th Annual Symposium of the IEEE Photonics Benelux Chapter 2023 Institute of Electrical and Electronics Engineers (2023).

[15] L. Sieben - Xu, "Monolithic Integrated Reflective Transceiver in Indium Phosphide," Eindhoven University of Technology (2009).